Correlation of antero-dorsal active contact location with weight gain after subthalamic nucleus deep brain stimulation: a case series

Katsuki Eguchi (k198762@gmail.com)
Department of Neurology, Faculty of Medicine and Graduate School of Medicine, Hokkaido University
Shinichi Shirai
Department of Neurology, Faculty of Medicine and Graduate School of Medicine, Hokkaido University
Masaaki Matsushima
Department of Neurology, Faculty of Medicine and Graduate School of Medicine, Hokkaido University
Takahiro Kano
Department of Neurology, Faculty of Medicine and Graduate School of Medicine, Hokkaido University
Kazuyoshi Yamazaki
Department of Neurosurgery, Faculty of Medicine and Graduate School of Medicine, Hokkaido University
Shuji Hamauchi
Department of Neurosurgery, Faculty of Medicine and Graduate School of Medicine, Hokkaido University
Toru Sasamori
Department of Neurosurgery, Sapporo Azabu Neurosurgical Hospital
Kenji Hirata
Department of Diagnostic Imaging, Faculty of Medicine and Graduate School of Medicine
Mayumi KItagawa
Sapporo Teishinkai Hospital
Mika Otsuki
Faculty of Health Sciences and Graduate School of Health Sciences, Hokkaido University
Tohru Shiga
Department of Nuclear Medicine, Faculty of Medicine and Graduate School of Medicine, Hokkaido University
Kiyohiro Houkin
Department of Neurosurgery, Faculty of Medicine and Graduate School of Medicine, Hokkaido University
Hidenao Sasaki
Department of Neurology, Faculty of Medicine and Graduate School of Medicine, Hokkaido University
Ichiro Yabe
Department of Neurology, Faculty of Medicine and Graduate School of Medicine, Hokkaido University

Research Article

Keywords: Deep brain stimulation, Parkinson's disease, subthalamic nucleus, weight gain

Posted Date: April 6th, 2021

DOI: https://doi.org/10.21203/rs.3.rs-384471/v1

Abstract

Background Weight gain is a frequently reported side effect of subthalamic deep brain stimulation; however, the underlying mechanisms remain unclear. The active contact locations influence the clinical outcomes of subthalamic deep brain stimulation, but it is unclear whether weight gain is directly associated with the active contact locations. We aimed to determine whether weight gain is associated with the subthalamic deep brain stimulation active contact locations.

Methods We enrolled 14 patients with Parkinson's disease who underwent bilateral subthalamic deep brain stimulation between 2013 and 2019. Bodyweight and body mass index were measured before and one year following surgery. The Lead-DBS Matlab toolbox was used to determine the active contact locations based on magnetic resonance imaging and computed tomography. Fluorodeoxyglucose-positron emission tomography data were also acquired before and one year following surgery, and statistical parametric mapping was used to evaluate changes in brain metabolism. The relationship between weight and active contact locations was evaluated with a Spearman rank test with a corrected p-value < 0.008. We examined which brain regions' metabolism fluctuation significantly correlated with increased BMI scores and PET data.

Results The body mass index increase was 2.03 kg/m^2 1 year post-surgery. Weight gain was correlated with anterior and dorsal locations of the left-side active contacts, as well as with lateral locations of the right-side active contacts. Furthermore, weight gain was correlated with increased metabolism in the left-side limbic and associative regions, including the middle temporal gyrus, inferior frontal gyrus, and orbital gyrus.

Conclusions Although the mechanisms underlying weight gain following subthalamic deep brain stimulation are possibly multifactorial, our findings suggest that anterior subthalamic deep brain stimulation alters the activities in the limbic and associative cortical regions, which may then lead to weight gain. Weight gain could be prevented by avoiding stimulation to the anterior part of the subthalamic nucleus.

Background

Subthalamic nucleus deep brain stimulation (STN-DBS) is an established and effective treatment strategy for advanced Parkinson's disease (PD) [1]. However, STN-DBS is associated with several adverse effects, of which weight gain (WG) is one of the most common, although the underlying mechanisms have not been fully elucidated. Previous reports have suggested that WG is associated with lowered resting energy needs [2, 3], fewer motor complications (especially dyskinesia) [4–6], changes in eating behaviors [7, 8], and hormonal factors [9, 10]. However, these factors do not completely explain WG, suggesting that WG following STN-DBS is a multifactorial process [11].

The locations of electrodes and active contacts affect the clinical outcomes and adverse effects of STN-DBS [12, 13]. Based on animal studies [14, 15] and studies examining the human brain using diffusion

tensor imaging [16–18], the STN is divided into three functional subregions: the sensorimotor, associative, and limbic regions. Previous studies have suggested that superior motor improvement is achieved by stimulating the sensorimotor area, which is located in the dorsolateral part of the STN and is linked to the primary motor and supplementary motor cortices [17, 19–21]. Nevertheless, an increased risk of neuropsychiatric side effects may be associated with stimulation of the limbic area, which exists in the anteromedial part of the STN [17, 22]. However, few studies have evaluated whether WG is directly correlated with the positions of the active contacts during STN-DBS. Therefore, this study prospectively evaluated patients who underwent STN-DBS for PD and aimed to determine whether WG was correlated with the positions of the active contacts. Moreover, we evaluated whether WG was associated with altered glucose metabolism in specific brain regions to estimate which functional subregion(s) influenced WG.

Materials And Methods

Patients

We aimed to determine whether WG is associated with the subthalamic deep brain stimulation active contact locations. This prospective study recruited PD patients who underwent bilateral STN-DBS surgery at Hokkaido University Hospital between 2013 and 2019. We recruited 16 patients with PD who underwent bilateral STN-DBS surgery, although we excluded one patient who withdrew from participating and another who required electrode removal that was related to an infection. Thus, this study analyzed data from 14 patients, including 12 women. The median age at DBS surgery was 62.5 (55.5–68) years, and the median disease duration at DBS surgery was 14.3 (12–20.5) years. The eligibility for DBS surgery was determined based on the guidelines of the International Parkinson and Movement Disorders Society [23].

This study was conducted following the 1964 Declaration of Helsinki and its later amendments and was approved by the ethics panel of the institutional review board of Hokkaido University Hospital. All patients provided written informed consent before their inclusion in the study.

Clinical assessment

Clinical assessments were conducted at the preoperative baseline and one year following surgery. Bodyweight and height were measured and used to calculate the body mass index (BMI, kg/m^2). Motor symptoms were assessed using the United Parkinson's Disease Rating Scale (UPDRS) part III in the MedOff state at baseline and in the MedOff and DBS-on state at one year following surgery. Dyskinesia was also evaluated using items 32 and 33 of the UPDRS part IV. Neuropsychological evaluations were based on the Mini Mental State Examination, Frontal Assessment Battery (FAB), Apathy Scale [24], and Patient Health Questionnaire-9 (PHQ-9) [25]. The levodopa-equivalent daily dose (LEDD) [26] was calculated at both baseline and one year following DBS surgery. Brain metabolism was evaluated using fluorodeoxyglucose-positron emission tomography (FDG-PET) at baseline and one year following surgery.

The DBS stimulation parameters were recorded after one year and included the stimulation voltage, pulse width, frequency, and active contact location.

Assessing the active contact positions

The active contact positions were evaluated using Lead-DBS, which is a validated Matlab toolbox [27, 28] that was implemented using Matlab 2019b (MathWorks, Natick, MA, USA). Preoperative results were obtained via T2-weighted magnetic resonance imaging (MRI, slice thickness: 1 mm; echo time; 222 ms; repetition time: 2,000 ms), and postoperative results were obtained via computed tomography (CT). The preoperative MRI and postoperative CT images were co-registered using advanced normalization tools [29] and then nonlinearly normalized into Montreal Neurological Institute (MNI) standard space (MNI_ICBM_2009b_NLIN_Asym). The DBS electrodes were automatically reconstructed using the TRAC/CORE algorithm [28] and manually refined to evaluate their coordinates in MNI space. If more than one contact was used for the stimulation, the mean coordinates of all active contacts were recorded. The positional relationships between the active contacts and the STN were assessed using the DISTAL atlas [30], which is a composite atlas that is based on histology, structural connectivity, and manual segmentations of a multimodal brain template that is normalized in MNI space.

FDG-PET acquisition and preprocessing

Patients were instructed to fast overnight before the PET scans. PET scans were performed in the MedOn at baseline and in the MedOn and DBS-off state post-operation. DBS stimulation was turned off 30–60 minutes before PET scans. ^{18}F-FDG (4.5 MBq/kg) was administered intravenously, and serum glucose was measured to exclude the patients showing fasting hyperglycemia (> 150 mg/dL). The images were acquired 60 min following FDG administration for 10-min emission scanning. Pet data were obtained using either a GEMINI TF64 (Philips, Amsterdam, Netherlands) PET-CT scanner or a Biograph 64 (Siemens, Munich, Germany) TruePoint PET-CT scanner for different patients. Time-of-flight technology was used with GEMINI TF64 but not with Biograph 64. Images were reconstructed using ordered subset expectation–maximization. The PET images were preprocessed using statistical parametric mapping (SPM12; Wellcome Department of Cognitive Neurology, London, UK) running on Matlab 2019b. The PET images were initially subjected to affine and nonlinear spatial normalization into the MNI brain space, although we used an FDG-PET-specific template that was described by Della Rosa et al [31] instead of the default $^{15}H_2O$-SPM template. The normalized images were then smoothed using an 8-mm isotropic Gaussian filter to compensate for individual anatomical variability. Finally, we created a percent signal change map (PSC map) using the following formula:

$$PSC = (V_{1y} - V_b) \times 100 / V_b,$$

where V_{1y} and V_b represent voxel values at one year following surgery and baseline, respectively.

Statistical analysis

Scores are reported as the median ± interquartile range (IQR), and nonparametric analyses were used based on the small sample size. Preoperative and postoperative values for BMI, UPDRS part III and IV

scores, neuropsychological data, and LEDD were compared using the Wilcoxon signed-rank test, and $p < 0.001$ was considered as statistically significant using Bonferroni correction. Stimulation voltage and active contact coordinates for the left and right sides were compared using Wilcoxon's rank-sum test. The correlation between WG after STN-DBS and the active contact positions (based on X-, Y-, and Z-axis coordinates on both sides) was evaluated using the Spearman rank test, and $p < 0.008$ was considered as statistically significant using Bonferroni correction. To detect potential confounders for WG other than the active contact positions, analyses were performed to determine the correlation between WG and preoperative BMI, improvement in the UPDRS part III and IV (items 32 + 33) scores, LEDD reduction, and stimulation voltage using the Spearman rank test ($p < 0.05$ was considered as significant). Statistical analyses were conducted using JMP Pro software (version 14; SAS Inc., Cary, North Carolina, USA).

The PET data were analyzed using SPM12 (Wellcome Department of Cognitive Neurology, London, UK). To identify which brain regions' metabolism change correlated significantly with increased BMI scores, a general linear model was tested at each voxel with the BMI score as a covariate using a PSC map. LEDD was included in the SPM analysis as a covariate, A voxel-level threshold of $P < 0.05$ (family-wise error corrected for multiple comparisons) was used to assess the SPM t values. If statistical significance was not reached, we performed the same analysis with a voxel-level threshold of $P < 0.005$ (uncorrected for multiple comparisons), considering the small sample size and the study's exploratory nature. Only clusters containing > 100 voxels were reported.

Results

Clinical outcomes

Table 1 shows the clinical values at preoperative baseline and one year following DBS surgery. A significant motor improvement was observed at 1-year post-surgery, based on the decreased UPDRS part III scores in the MedOff state. A non-significant trend toward decreased values for items 32 and 33 of the UPDRS part IV was also observed. Bodyweight and BMI values increased significantly following STN-DBS. The neuropsychological assessments revealed a small but statistically significant increase in the FAB score but no significant changes in the other scales. There was a non-significant trend toward decreasing LEDD after DBS surgery.

Table 1
Clinical values at baseline and 1-year follow-up

	Baseline	1-year Follow-up	p-value
Bodyweight	55.8 (49.7–63.6)	60.7 (53.1–69.6)	< 0.001
BMI	23.1 (20.1–25.7)	24.5 (22.0–29.1)	< 0.001
UPDRS part III (MedOn)	14 (10–18)	8 (4.5–19.3)	0.13
UPDRS part III (MedOff)	40 (33.8–44.3)	16 (11.8–23)	< 0.001
UPDRS part IV (items 32 + 33)	1.5 (0–4)	1 (0–2.25)	0.12
MMSE	29 (27.8–30)	29 (28–30)	0.3
FAB	14.5 (14.5–17.5)	15.5 (13.8–17.3)	0.023
Apathy scale	13.5 (7.5–16)	14 (4.8–16.3)	0.47
PHQ-9	5 (4–8)	4 (0–7.8)	0.43
LEDD	689 (363–748.5)	418.5 (297.3–656.3)	0.085
Scores are reported as the median (interquartile range)			
BMI: body mass index; FAB: Frontal Assessment Battery; LEDD: levodopa-equivalent daily dose; Medoff: a condition without intaking medication; MedOn: a condition requiring intaking medication. MMSE: Mini Mental State Examination; PHQ-9; Patient Health Questionnaire-9; UPDRS: Unified Parkinson's Disease Rating Scale.			

Stimulation parameters and active contact positions

All patients received bilaterally implanted quadripolar (from contact number '0' for the most ventral contact to '3' for the most dorsal one) DBS electrodes (3387; Medtronic, Minneapolis, MN, USA). Each patient's stimulation parameters at one year following DBS surgery are shown in Table 2. The stimulation intensities were similar between the right and left sides. Figure 1 shows the electrode locations for all patients regarding the STN as defined using the DISTAL atlas and MNI space. The median coordinates of the right-side active contacts were 12.5 (11.7–13.5) mm on the X-axis, − 14.5 (−13.7 - − 14.5) mm on the Y-axis, and − 6.4 (−5.6 - − 7.6) mm on the Z-axis. The mean left-side coordinates were − 13.6 (−11.5 - − 14.2) mm on the X-axis, − 13.6 (−11.8 - − 15.6) mm on the Y-axis, and − 6.8 (−5.1 - − 6.9) mm on the Z-axis. The X-, Y-, and Z-axis coordinates were not significantly different between the right and left sides, although the left-side Y-axis coordinates had a larger IQR than the right-side Y-axis coordinates.

Table 2
BMI change from baseline and stimulation parameters at one year following surgery

	Change in body mass index from baseline	Active contacts		Frequency (Hz)		Voltage (V)		Pulse width (μs)	
Participant No.		Right	Left	Right	Left	Right	Left	Right	Left
1	2.3	C(+)1(-)2(-)	C(+)2(-)	130	130	1.5	2.2	60	60
2	3.8	C(+)1(-)	C(+)2(-)	130	130	1.2	1.2	60	60
3	3.2	C(+)1(-)2(-)	C(+)2(-)	130	130	2.6	1.8	60	60
4	1.0	C(+)3(-)	C(+)3(-)	130	130	1	1	60	60
5	-0.2	C(+)1(-)	C(+)1(-)	130	130	1	2	60	60
6	-0.2	C(+)2(-)	0(+)1(-)	130	130	2.8	3.2	60	150
7	4.6	C(+)2(-)	C(+)2(-)	60	60	2.2	3.7	60	90
8	1.3	1(+)2(-)	C(+)2(-)	130	130	3.4	3.2	150	90
9	2.8	C(+)2(-)	C(+)3(-)	130	130	3	3	60	60
10	3.7	C(+)2(-)	C(+)2(-)	130	130	2.8	2.8	90	90
11	0.7	C(+)2(-)	C(+)2(-)	130	130	1.4	1.4	90	90
12	2.4	C(+)2(-)	C(+)2(-)	130	130	2.1	1.7	60	60
13	2.3	C(+)1(-)	C(+)2(-)	130	130	1.8	3	60	60
14	0.7	C(+)2(-)	C(+)1(-)	130	130	1.9	2	60	60

Correlations with increased BMI

On the left side, WG was significantly correlated with the Y-axis coordinates (r = 0.77, $P = 0.001$) and the Z-axis coordinates (r = 0.77, $P < 0.001$), which suggests that WG was associated with contacts located more anteriorly and dorsally within the STN (Fig. 2). WG was not significantly correlated with the active contact coordinates on the left-side X-axis, right-side X-axis, Y-axis, and Z-axis. Preoperative BMI, improvements in the UPDRS part III and IV scores, LEDD reduction, and stimulation voltage also did not correlate with WG.

PET image analysis

We analyzed PET data from 13 patients since one patient's PET data were missing. A GEMINI TF64 PET-CT scanner was used for 12 patients, while a Biograph 64 TruePoint PET-CT scanner was used for the

remaining patient. None of the voxels were significant at a voxel-level threshold of $P < 0.05$ (family-wise error corrected for multiple comparisons). However, at a threshold of $P < 0.005$ (uncorrected for multiple comparisons), we identified several clusters with positive correlations between WG and increased metabolism in the left hemisphere (Table 3 and Fig. 3). The correlations were observed in the left middle temporal gyrus, inferior frontal gyrus, lateral orbital gyrus, anterior orbital gyrus, and planum polare. We did not observe any negative correlations between WG and brain metabolism in the various areas.

Table 3
Correlations between weight gain and increased brain metabolism at various locations

	Coordinates				
Region	X	Y	Z	Peak T value	No. of Voxels
Left middle temporal gyrus	-68	-16	-20	6.8	575
Left triangular part of the inferior frontal gyrus	-34	32	2	6.26	401
Left lateral orbital gyrus	-44	32	-16	4.83	734
Left anterior orbital gyrus	-32	62	-10	4.11	103
Left planum polare	-42	-12	-8	4	107
The uncorrected thresholds were significant ($P < 0.005$) at the voxel level. Only clusters with > 100 voxels are reported.					

Discussion

This study showed a mean BMI increase of 2 kg/m^2 at one year following DBS surgery, which agrees with previous findings [32]. Furthermore, the mean active contact coordinates in our study were similar to the preferred coordinates for motor improvement from previous studies [33]. Moreover, WG after STN-DBS was significantly correlated with some active contact coordinates and with increased glucose metabolism in the left frontal and temporal lobes. We could not detect a significant correlation between WG and dyskinesia reduction, while previous findings remain conflicting [4–6, 33].

The STN plays an important role in reward processing [34], and several studies have indicated that the STN is involved in controlling appetite and eating behavior. For example, a study on non-human primates illustrated that STN activity increased during food reward anticipation and delivery [35]. In humans, stroke or tumors affecting the STN causes hyperphagia and increases appetite [36, 37], while abnormal eating behaviors have been reported following STN-DBS [7, 38–42]. The anteromedial part of the STN is thought to be involved in reward and emotion processing, and dysfunction in this area can induce stereotyped and violent behaviors in non-human primates [43]. Moreover, during STN-DBS, stimulation of the anteromedial part of the STN led to an increased risk of abnormal behavior [22, 44, 45]. Considering these

findings, our results regarding the correlation between WG and anterior active contact locations suggest that WG is associated with the stimulation of the anteromedial part of the STN.

We observed correlations between WG and increased metabolism in the limbic and associative areas but not the sensorimotor areas; however, these were not statistically significant in multiple comparisons. A previous FDG-PET study showed that WG after STN-DBS was correlated with increased metabolism in the limbic and associative regions, including the orbitofrontal cortex, lateral and medial parts of the temporal lobe, anterior cingulate cortex, and retrosplenial cortex [33]. Other PET and functional MRI studies have also suggested that a broad network of limbic and paralimbic network structures mediates the desire for food [46–53]. This network is thought to integrate sensory information with the cognitive desire for food and induces behaviors that aim to obtain food [54, 55]. Regions with increased brain metabolism in our study were also associated with the processing of desire for food, which suggests that stimulating the anterior part of the STN changed the activities in the limbic and associative areas, which modified food-related behavior and ultimately WG. Nevertheless, a larger prospective study with correction for multiple comparisons is warranted to confirm this hypothesis.

We also observed that WG was correlated with the left-side active contact Z-axis coordinates, which agrees with a previous report indicating that active contacts located in the zona incerta (dorsally out of the STN) were correlated with increased appetite after STN-DBS [56]. The zona incerta contains neurons expressing melanin-concentrating hormone, which is involved in the regulation of feeding [57]. Thus, our finding of a correlation between WG and the Z-axis coordinates might be explained by the stimulation of zona incerta and neurons that express melanin-concentrating hormone. However, dorsally located contacts are usually also located anteriorly, since the DBS electrodes are usually inserted from the anterodorsal aspect to the posteroventral aspect. Thus, the Y- and Z-axis coordinates acted as confounders for each other. To determine which direction of current spread to the anterior part of STN or Zi is more important for WG, we need to conduct further studies.

We observed that WG was correlated with active contact locations and increased brain metabolism only on the left side. Several studies have also indicated that unilateral STN-DBS causes WG [58, 59], although the laterality of this relationship remains unclear. In this study, left-side active contact Y-axis coordinates had a larger IQR value than the right-side coordinates; the greater variability in the left-side coordinates may explain the laterality of our FDG-PET findings. However, further studies are warranted to determine whether stimulating the right-side anterior part of the STN could influence brain metabolism, subsequently causing WG.

This study has several limitations. First, we did not assess eating habits or daily food intake. Thus, future studies must confirm whether WG is caused by stimulation of the limbic area, which induced changes in eating behaviors, using preoperative and postoperative data on eating behaviors and food intake. Second, we did not assess hormonal factors or swallowing function, which could have confounded our analyses. Third, although we measured the active contact coordinates, we did not assess the volume of tissue activation (VTA) or connectivity between the stimulation site and brain regions. Recent studies

have indicated that the clinical outcomes of DBS could be predicted based on the connectivity profile of the VTA and cortical areas [60, 61]. Therefore, the association between WG and stimulation of the limbic area should be confirmed by analyzing the connectivity between the VTA and cortical area. Fourth, we obtained PET data only in an “off DBS” state after the surgery. Therefore, it is difficult to attribute the changes in brain metabolism after DBS to the plasticity of the neural circuit or the washout process of therapeutic DBS.

Conclusion

In conclusion, we found that WG was correlated with active contact coordinates on several axes. Since WG is likely a multifactorial process, it is difficult to determine which axes might have the greatest effects. However, based on our PET findings, WG might be associated with stimulating more anteriorly within the STN and subsequent changes in eating behaviors. Further investigations are warranted to confirm this hypothesis by accurately assessing eating behaviors and food intake.

List Of Abbreviations

BMI: Body mass index; CT: Computed tomography; FAB: Frontal Assessment Battery; LEDD: Levodopa-equivalent daily dose; MMSE: Mini Mental State Examination; MNI: Montreal Neurological Institute; MRI: Magnetic resonance imaging; PD: Parkinson’s disease; PHQ-9: Patient Health Questionnaire-9; PSC: Percent signal change; UPDRS: United Parkinson’s Disease Rating Scale; VTA: Volume of tissue activation; WG: Weight gain

Declarations

Ethics approval and consent to participate

This study was conducted following the 1964 Declaration of Helsinki and its later amendments and was approved by the institutional review board of Hokkaido University Hospital. All patients provided written informed consent prior to their inclusion in the study.

Consent for publication

Not applicable

Availability of data and materials

The dataset(s) used and/or analyzed during the current study are available from the corresponding author on reasonable request.

Competing interests

The authors declare that they have no competing interests.

Funding

This work was supported in part by a Grant-in-Aid for the Research Committee of CNS Degenerative Diseases under Research on Measures for Intractable Diseases from the Ministry of Health, Welfare, and Labour, Japan [grant number 20FC1049].

Authors' contributions

Examination and treatment of Parkinson disease: K. Eguchi, S. Shirai, M. Matsushima, T. Kano, K. Yamazaki, S. Hamauchi, T. Sasamori, T. Seki, and Yabe I.

PET data acquisition and analysis: K. Hiraka and T. Shiga.

Neuropsychological assessment: M. Otsuki.

Drafting of the manuscript: K. Eguchi.

Critical revision of the manuscript for important intellectual content: I. Yabe.

Supervision: M. Kitagawa, K. Houkin, and H. Sasaki.

Acknowledgments

We thank Ms. Megumi Takeuchi for performing the neuropsychological examinations.

References

1. Krack P, Batir A, Van Blercom N, Chabardes S, Fraix V, Ardouin C, et al. Five-year follow-up of bilateral stimulation of the subthalamic nucleus in advanced Parkinson's disease. N Engl J Med. 2003;349:1925-34.
2. Montaurier C, Morio B, Bannier S, Derost P, Arnaud P, Brandolini-Bunlon M, et al. Mechanisms of body weight gain in patients with Parkinson's disease after subthalamic stimulation. Brain. 2007;130:1808-18.
3. Jorgensen HU, Werdelin L, Lokkegaard A, Westerterp KR, Simonsen L. Free-living energy expenditure reduced after deep brain stimulation surgery for Parkinson's disease: Decreased energy expenditure after STN-DBS surgery. Clin Physiol Funct Imaging. 2012;32:214-20.
4. Gironell A, Pascual-Sedano B, Otermin P, Kulisevsky J. Weight gain after functional surgery for Parkinsons disease. Neurologia. 2002;17:310-6.
5. Barichella M, Marczewska AM, Mariani C, Landi A, Vairo A, Pezzoli G. Body weight gain rate in patients with Parkinson's disease and deep brain stimulation. Mov Disord. 2003;18:1337-40.
6. Balestrino R, Baroncini D, Fichera M, Donofrio CA, Franzin A, Mortini P, et al. Weight gain after subthalamic nucleus deep brain stimulation in Parkinson's disease is influenced by dyskinesias' reduction and electrodes' position. Neurol Sci. 2017;38:2123-9.

7. Zahodne LB, Susatia F, Bowers D, Ong TL, Jacobson CE 4th, Okun MS, et al. Binge eating in Parkinson's disease: prevalence, correlates and the contribution of deep brain stimulation. J Neuropsychiatry Clin Neurosci. 2011;23:56-62.
8. Amami P, Dekker I, Piacentini S, Ferré F, Romito LM, Franzini A, et al. Impulse control behaviours in patients with Parkinson's disease after subthalamic deep brain stimulation: de novo cases and 3-year follow-up. J Neurol Neurosurg Psychiatry. 2015;86:562-4.
9. Guimarães J, Moura E, Vieira-Coelho MA, Garrett C. Weight variation before and after surgery in Parkinson's disease: a noradrenergic modulation? Mov Disord. 2012;27:1078-82.
10. Seifried C, Boehncke S, Heinzmann J, Baudrexel S, Weise L, Gasser T, et al. Diurnal variation of hypothalamic function and chronic subthalamic nucleus stimulation in Parkinson's disease. Neuroendocrinology. 2013;97:283-90.
11. Rieu I, Derost P, Ulla M, Marques A, Debilly B, De Chazeron I, et al. Body weight gain and deep brain stimulation. J Neurol Sci. 2011;310:267-70.
12. Tripoliti E, Zrinzo L, Martinez-Torres I, Tisch S, Frost E, Borrell E, et al. Effects of contact location and voltage amplitude on speech and movement in bilateral subthalamic nucleus deep brain stimulation. Mov Disord. 2008;23:2377-83.
13. Bot M, Schuurman PR, Odekerken VJJ, Verhagen R, Contarino FM, De Bie RMA, et al. Deep brain stimulation for Parkinson's disease: defining the optimal location within the subthalamic nucleus. J Neurol Neurosurg Psychiatry. 2018;89:493-8.
14. Karachi C, Yelnik J, Tandé D, Tremblay L, Hirsch EC, François C. The pallidosubthalamic projection: an anatomical substrate for nonmotor functions of the subthalamic nucleus in primates. Mov Disord. 2005;20:172-80.
15. Haynes WIA, Haber SN. The organization of prefrontal-subthalamic inputs in primates provides an anatomical substrate for both functional specificity and integration: implications for Basal Ganglia models and deep brain stimulation. J Neurosci. 2013;33:4804-14.
16. Lambert C, Zrinzo L, Nagy Z, Lutti A, Hariz M, Foltynie T, et al. Confirmation of functional zones within the human subthalamic nucleus: Patterns of connectivity and sub-parcellation using diffusion weighted imaging. Neuroimage. 2012;60:83-94.
17. Accolla EA, Dukart J, Helms G, Weiskopf N, Kherif F, Lutti A, et al. Brain tissue properties differentiate between motor and limbic basal ganglia circuits. Hum Brain Mapp. 2014;35:5083-92.
18. Plantinga BR, Temel Y, Duchin Y, Uludağ K, Patriat R, Roebroeck A, et al. Individualized parcellation of the subthalamic nucleus in patients with Parkinson's disease with 7T MRI. Neuroimage. 2018;168:403-11.
19. Eisenstein SA, Koller JM, Black KD, Campbell MC, Lugar HM, Ushe M, et al. Functional anatomy of subthalamic nucleus stimulation in Parkinson disease: STN DBS Location and PD. Ann Neurol. 2014;76:279-95.
20. Akram H, Sotiropoulos SN, Jbabdi S, Georgiev D, Mahlknecht P, Hyam J, et al. Subthalamic deep brain stimulation sweet spots and hyperdirect cortical connectivity in Parkinson's disease.

Neuroimage. 2017;158:332-45.
21. Gourisankar A, Eisenstein SA, Trapp NT, Koller JM, Campbell MC, Ushe M, et al. Mapping movement, mood, motivation and mentation in the subthalamic nucleus. R Soc Open Sci. 2018;5:171177.
22. Castrioto A, Lhommée E, Moro E, Krack P. Mood and behavioural effects of subthalamic stimulation in Parkinson's disease. Lancet Neurol. 2014;13:287-305.
23. Lang AE, Houeto J-L, Krack P, Kubu C, Lyons KE, Moro E, et al. Deep brain stimulation: preoperative issues. Mov Disord. 2006;21 Suppl 14:S171-96.
24. Starkstein SE, Fedoroff JP, Price TR, Leiguarda R, Robinson RG. Apathy following cerebrovascular lesions. Stroke. 1993;24:1625-30.
25. Kroenke K, Spitzer RL, Williams JB. The PHQ-9: validity of a brief depression severity measure. J Gen Intern Med. 2001;16:606-13.
26. Tomlinson CL, Stowe R, Patel S, Rick C, Gray R, Clarke CE. Systematic review of levodopa dose equivalency reporting in Parkinson's disease. Mov Disord. 2010;25:2649-53.
27. Horn A, Kühn AA. Lead-DBS: A toolbox for deep brain stimulation electrode localizations and visualizations. Neuroimage. 2015;107:127-35.
28. Horn A, Li N, Dembek TA, Kappel A, Boulay C, Ewert S, et al. Lead-DBS v2: Towards a comprehensive pipeline for deep brain stimulation imaging. Neuroimage. 2019;184:293-316.
29. Avants BB, Epstein CL, Grossman M, Gee JC. Symmetric diffeomorphic image registration with cross-correlation: evaluating automated labeling of elderly and neurodegenerative brain. Med Image Anal. 2008;12:26-41.
30. Ewert S, Plettig P, Li N, Chakravarty MM, Collins DL, Herrington TM, et al. Toward defining deep brain stimulation targets in MNI space: A subcortical atlas based on multimodal MRI, histology and structural connectivity. Neuroimage. 2018;170:271-82.
31. Della Rosa PA, and the EADC-PET Consortium, Cerami C, Gallivanone F, Prestia A, Caroli A, et al. A standardized [18F]-FDG-PET template for spatial normalization in statistical parametric mapping of dementia. Neuroinformatics. 2014;12:575-93.
32. Bannier S, Montaurier C, Derost PP, Ulla M, Lemaire J-J, Boirie Y, et al. Overweight after deep brain stimulation of the subthalamic nucleus in Parkinson disease: long term follow-up. J Neurol Neurosurg Psychiatry. 2009;80:484-8.
33. Sauleau P, Le Jeune F, Drapier S, Houvenaghel J-F, Dondaine T, Haegelen C, et al. Weight gain following subthalamic nucleus deep brain stimulation: a PET study. Mov Disord. 2014;29:1781-7.
34. Rossi PJ, Gunduz A, Okun MS. The subthalamic nucleus, limbic function, and impulse control. Neuropsychol Rev. 2015;25:398-410.
35. Espinosa-Parrilla J-F, Baunez C, Apicella P. Modulation of neuronal activity by reward identity in the monkey subthalamic nucleus. Eur J Neurosci. 2015;42:1705-17.
36. Barutca S, Turgut M, Meydan N, Ozsunar Y. Subthalamic nucleus tumor causing hyperphagia--case report. Neurol Med Chir (Tokyo). 2003;43:457-60.

37. Etemadifar M, Abtahi SH, Abtahi SM, Mirdamadi M, Sajjadi S, Golabbakhsh A, et al. Hemiballismus, hyperphagia, and behavioral changes following subthalamic infarct. Case Rep Med. 2012;2012:768580.
38. Aiello M, Eleopra R, Rumiati RI. Body weight and food intake in Parkinson's disease. A review of the association to non-motor symptoms. Appetite. 2015;84:204-11.
39. Ardouin C, Voon V, Worbe Y, Abouazar N, Czernecki V, Hosseini H, et al. Pathological gambling in Parkinson's disease improves on chronic subthalamic nucleus stimulation. Mov Disord. 2006;21:1941-6.
40. Kistner A, Lhommée E, Krack P. Mechanisms of body weight fluctuations in Parkinson's disease. Front Neurol. 2014;5:84.
41. Lim SY, O'Sullivan SS, Kotschet K, Gallagher DA, Lacey C, Lawrence AD, et al. Dopamine dysregulation syndrome, impulse control disorders and punding after deep brain stimulation surgery for Parkinson's disease. J Clin Neurosci. 2009;16:1148-52.
42. Witjas T, Baunez C, Henry JM, Delfini M, Regis J, Cherif AA, et al. Addiction in Parkinson's disease: impact of subthalamic nucleus deep brain stimulation. Mov Disord. 2005;20:1052-5.
43. Karachi C, Grabli D, Baup N, Mounayar S, Tandé D, François C, et al. Dysfunction of the subthalamic nucleus induces behavioral and movement disorders in monkeys. Mov Disord. 2009;24:1183-92.
44. Krack P, Kumar R, Ardouin C, Dowsey PL, McVicker JM, Benabid AL, et al. Mirthful laughter induced by subthalamic nucleus stimulation. Mov Disord. 2001;16:867-75.
45. Mallet L, Schüpbach M, N'Diaye K, Remy P, Bardinet E, Czernecki V, et al. Stimulation of subterritories of the subthalamic nucleus reveals its role in the integration of the emotional and motor aspects of behavior. Proc Natl Acad Sci U S A. 2007;104:10661-6.
46. Rothemund Y, Preuschhof C, Bohner G, Bauknecht H-C, Klingebiel R, Flor H, et al. Differential activation of the dorsal striatum by high-calorie visual food stimuli in obese individuals. Neuroimage. 2007;37:410-21.
47. Führer D, Zysset S, Stumvoll M. Brain activity in hunger and satiety: an exploratory visually stimulated FMRI study. Obesity (Silver Spring). 2008;16:945-50.
48. Killgore WDS, Young AD, Femia LA, Bogorodzki P, Rogowska J, Yurgelun-Todd DA. Cortical and limbic activation during viewing of high- versus low-calorie foods. Neuroimage. 2003;19:1381-94.
49. Siep N, Roefs A, Roebroeck A, Havermans R, Bonte ML, Jansen A. Hunger is the best spice: an fMRI study of the effects of attention, hunger and calorie content on food reward processing in the amygdala and orbitofrontal cortex. Behav Brain Res. 2009;198:149-58.
50. Goldstone AP, Prechtl de Hernandez CG, Beaver JD, Muhammed K, Croese C, Bell G, et al. Fasting biases brain reward systems towards high-calorie foods. Eur J Neurosci. 2009;30:1625-35.
51. Wallner-Liebmann S, Koschutnig K, Reishofer G, Sorantin E, Blaschitz B, Kruschitz R, et al. Insulin and hippocampus activation in response to images of high-calorie food in normal weight and obese adolescents. Obesity (Silver Spring). 2010;18:1552-7.

52. Wang G-J, Volkow ND, Telang F, Jayne M, Ma J, Rao M, et al. Exposure to appetitive food stimuli markedly activates the human brain. Neuroimage. 2004;21:1790-7.
53. Carnell S, Gibson C, Benson L, Ochner CN, Geliebter A. Neuroimaging and obesity: current knowledge and future directions. Obes Rev. 2012;13:43-56.
54. Tataranni PA, DelParigi A. Functional neuroimaging: a new generation of human brain studies in obesity research. Obes Rev. 2003;4:229-38.
55. Abizaid A, Horvath TL. Brain circuits regulating energy homeostasis. Regul Pept. 2008;149:3-10.
56. de Chazeron I, Pereira B, Chereau-Boudet I, Durif F, Lemaire JJ, Brousse G, et al. Impact of localisation of deep brain stimulation electrodes on motor and neurobehavioural outcomes in Parkinson's disease. J Neurol Neurosurg Psychiatry. 2016;87:758-66.
57. Adamantidis A, de Lecea L. Sleep and metabolism: shared circuits, new connections. Trends Endocrinol Metab. 2008;19:362-70.
58. Walker HC, Lyerly M, Cutter G, Hagood J, Stover NP, Guthrie SL, et al. Weight changes associated with unilateral STN DBS and advanced PD. Parkinsonism Relat Disord. 2009;15:709-11.
59. Lee EM, Kurundkar A, Cutter GR, Huang H, Guthrie BL, Watts RL, et al. Comparison of weight changes following unilateral and staged bilateral STN DBS for advanced PD. Brain Behav. 2011;1:12-8.
60. Horn A, Reich M, Vorwerk J, Li N, Wenzel G, Fang Q, et al. Connectivity predicts deep brain stimulation outcome in Parkinson disease. Ann Neurol. 2017;82:67-78.
61. Li N, Baldermann JC, Kibleur A, Treu S, Akram H, Elias GJB, et al. A unified connectomic target for deep brain stimulation in obsessive-compulsive disorder. Nat Commun. 2020;11:3364.

Figures

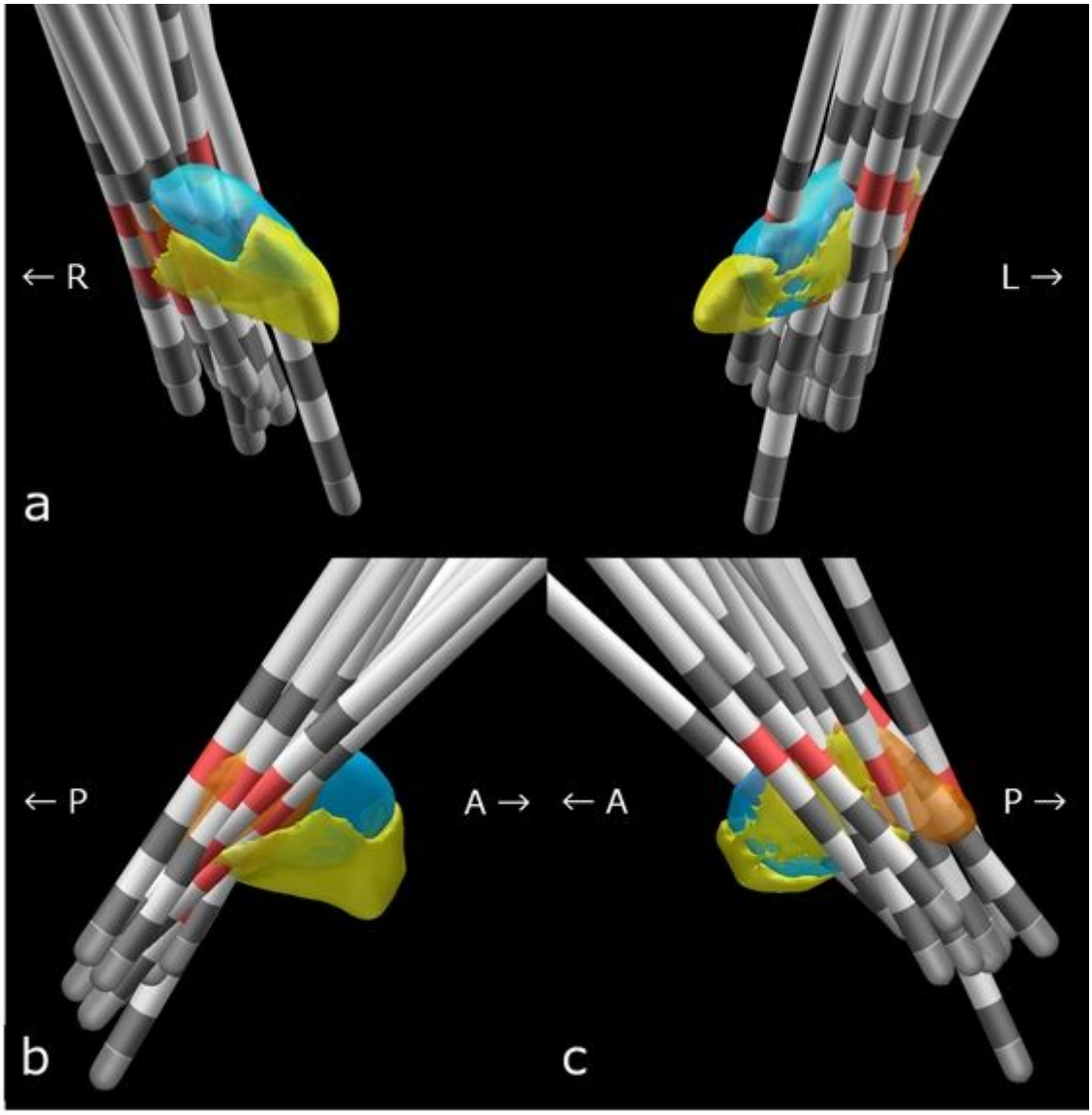

Figure 1

(a) Anterior view of the bilateral lead locations for all patients as well as the subthalamic nucleus (STN), as defined using the DISTAL atlas in Montreal Neurological Institute space. The functional subregions of the STN are highlighted (sensorimotor STN in copper, associative STN in blue, and limbic STN in yellow). The lateral views are shown for the right STN (b) and the left STN (c). Active contacts are highlighted in red. R, right; L, left; A, anterior; P, posterior

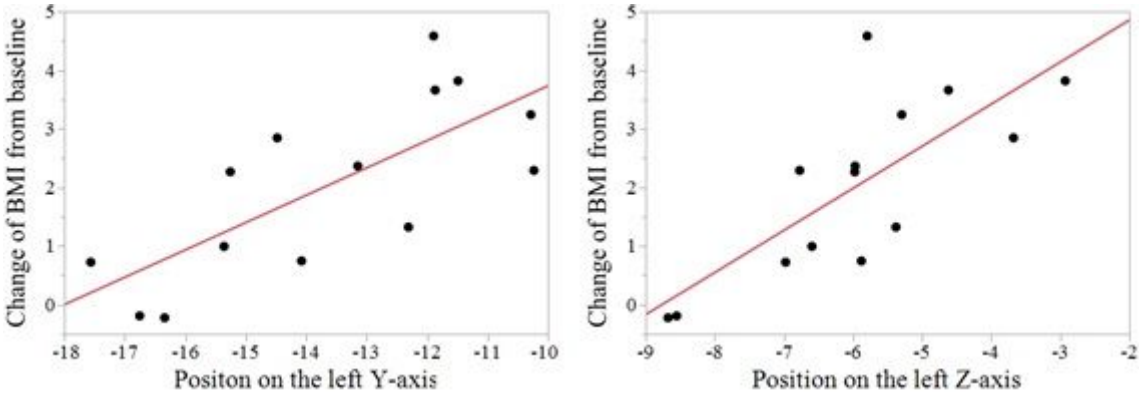

Figure 2

Correlations between WG and electrode position on the left Y-axis and Z-axis (correlation coefficient 0.77 and 0.77; p = 0.001 and < 0.001, respectively)

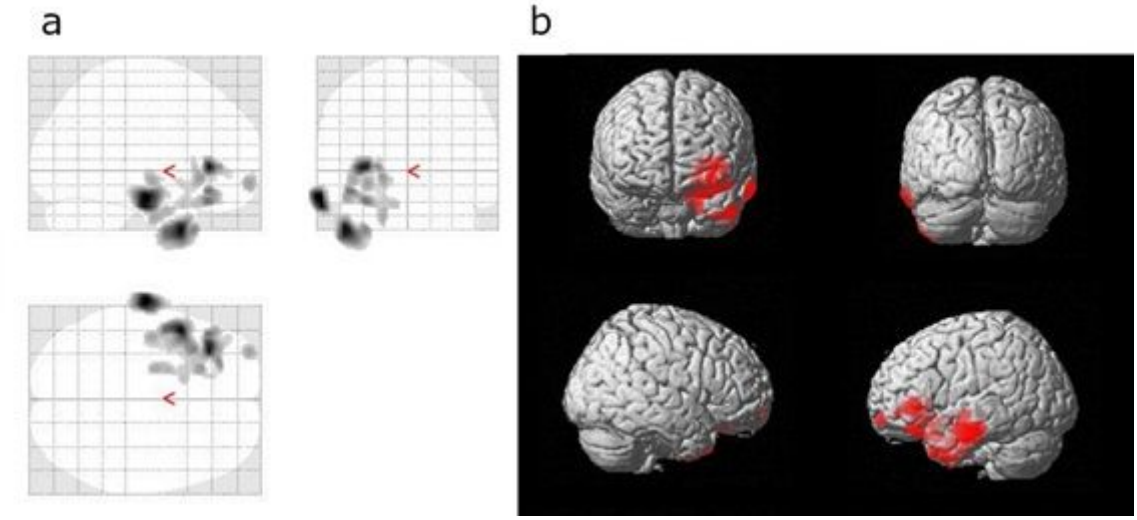

Figure 3

Positive correlations between weight gain and brain metabolism detected using fluorodeoxyglucose-positron emission tomography based on three orthogonal views (a) and a three-dimensional brain surface projection (b)